haematologica
Journal of the Ferrata Storti Foundation

Cd39 and P2rx7-Wnt signaling enhance blast pathogenicity in an experimental model of acute myeloid leukemia

by Lili Feng, Haohai Zhang, Changchuin Mao, Paola de Andrade Mello, Dina Stroopinsky, Eva Csizmadia, Jialin Zhou, David Avigan, Jinming Yu, Wenda Gao, and Simon C. Robson

Received: March 29, 2024.
Accepted: August 6, 2024.

Citation: Lili Feng, Haohai Zhang, Changchuin Mao, Paola de Andrade Mello, Dina Stroopinsky, Eva Csizmadia, Jialin Zhou, David Avigan, Jinming Yu, Wenda Gao, and Simon C. Robson. Cd39 and P2rx7-Wnt signaling enhance blast pathogenicity in an experimental model of acute myeloid leukemia.
Haematologica. 2024 Aug 15. doi: 10.3324/haematol.2024.285547 [Epub ahead of print]

Cd39 and P2rx7-Wnt signaling enhance blast pathogenicity in an experimental model of acute myeloid leukemia

Authors

Lili Feng,[1,2] Haohai Zhang,[1] Changchuin Mao,[3,4] Paola de Andrade Mello,[1] Dina Stroopinsky,[5] Eva Csizmadia,[1] Jialin Zhou,[6] David Avigan,[5] Jinming Yu,[6] Wenda Gao,[3,4#] & Simon C. Robson[1, 7#]

[1]Center for Inflammation Research, Department of Anesthesia, Critical Care & Pain Medicine, Beth Israel Deaconess Medical Center, Harvard Medical School, Boston, MA, USA; [2]Department of Hematology, Shandong Cancer Hospital and Institute, Shandong First Medical University and Shandong Academy of Medical Sciences, Jinan, Shandong, 250117, P. R. China; [3]Antagen Institute for Biomedical Research, Canton, MA, USA; [4]Antagen Pharmaceuticals, Inc. Canton, MA, USA; [5]Department of Bone Marrow Transplantation, Beth Israel Deaconess Medical Center, Harvard Medical School, Boston, MA, USA; [6]Department of Radiation Oncology, Shandong Cancer Hospital and Institute, Shandong First Medical University and Shandong Academy of Medical Sciences, Jinan, Shandong, 250117, P. R. China; [7]Department of Medicine, Division of Gastroenterology/Hepatology, Beth Israel Deaconess Medical Center, Harvard Medical School, Boston, MA, USA

[#]WG and SCR contributed equally as co-corresponding authors.

Correspondence: Wenda Gao, Antagen Pharmaceuticals, Inc., 780 Dedham St., STE 800, Canton, MA 02021, USA; e-mail: wendagao01@gmail.com;

Simon C. Robson, Department of Anesthesia, Critical Care & Pain Medicine, Division of Gastroenterology/Hepatology, Department of Medicine, Beth Israel Deaconess Medical Center, Harvard Medical School, CLS 612, 330 Brookline Avenue, Boston 02215, USA; e-mail: srobson@bidmc.harvard.edu.

Disclosures

WG is the founder and directs the Antagen Institute for Biomedical Research.

SCR is a scientific founder of Purinomia Biotech Inc and has consulted for eGenesis and SynLogic Inc; his interests are reviewed and managed by HMFP at Beth Israel Deaconess Medical Center in accordance with the conflict-of-interest policies.
The remaining authors declare no competing financial interests.

Contributions

SCR, LF and WG conceptualized the experimental study and interpreted data. LF, HZ, and WG developed the methodology. LF, HZ, CM, PM, DS, EC, and JZ carried out the investigation. LF wrote the original draft of the manuscript. WG and SCR reviewed and edited the manuscript. LF and WG generated figures. SCR, DA, JY and LF acquired funding. SCR and WG provided resources. DA and SCR jointly supervised the study.

Funding

This research was supported by the National Institute of Health (R01 DK108894; R21 CA164970 to SR and R21 CA221702 to both SR and DA) and Department of Defense Award W81XWH-16-0464 (to SR); the National Natural Science Foundation of China (82030082, 82002719 and 82172676) and the Natural Science Foundation of Shandong (ZR2021YQ52 and ZR2023MH233), together with scholarship awards from the China Scholarship Council to LF.

Data Sharing

The data supporting the findings of this study are available within the article and the appended supplementary materials. Data sets and sequence information presented in this study can be accessed through the NCBI home page at https://www.ncbi.nlm.nih.gov. under accession numbers SUB14589598. Other original data and full experimental protocols are immediately available to other investigators, with reasonable restrictions, from the corresponding authors [SCR and WG]. Additional data that support the findings of this study are available on request from the corresponding authors [SCR and WG], in agreement with the Data Management and Sharing (DMS) policy (NIH).

Acute myeloid leukemia (AML) is the most common type of acute leukemia in adults and is caused by uncontrolled clonal expansion of immature myeloid cells. Elements of the leukemic microenvironment, as well as blast cell- genetic and metabolic alterations, are all linked to adverse outcomes. [1] High CD39 expression on leukemic blast cells is associated with poor prognosis in AML patients.[2] CD39/ENTPD1 (ectonucleoside triphosphate diphosphohydrolase-1), in tandem with CD73, converts extracellular adenosine triphosphate (eATP) and adenosine diphosphate (eADP) to ultimately generate adenosine (eADO).[3] Extracellular nucleotides drive type-2 purinergic receptor (e.g. P2RX7) responses that underpin tumor immunity.[4] Genetic, pharmacological and immunological studies have documented the therapeutic potential of targeting CD39 and purinergic responses in solid tumors.[5-8] In this current work, we have explored the pathogenetic roles of Cd39 and P2rx7 and demonstrate novel down-stream elements of purinergic signaling in an experimental model of AML. Animal experimentation protocols were reviewed and approved by the IACUC of Beth Israel Deaconess Medical Center.

We established an aggressive AML model by transplanting TIB-49 cells into immunocompetent syngeneic C57BL/6 wild type (WT) mice. Heterogeneous expression patterns of Cd39 on immune cells throughout control mice and TIB-49-bearing mice blood, spleen and BM were revealed (Supplementary Figure S1A). TIB-49 cells from spleen and BM displayed high levels of Cd39 (Figure 1A), even though this was not detected on cultured TIB-49 cells *in vitro* (Supplementary Figure S1B). Furthermore, there were no Cd39 transcripts present in TIB-49 cells sorted from spleen and BM of WT AML mice (Supplementary Figure S1C).

We considered that TIB-49 cells acquired Cd39 via trogocytosis in specialized niches (e.g. spleen and BM) *in vivo*. To test this, TIB-49 cells were inoculated into *Cd39*$^{-/-}$ mice. We noted that these TIB-49 cells from *Entpd1* null blood, spleen and BM did not express Cd39 (Figure 1A). These data indicated that Cd39 on TIB-49 cells was acquired from Cd39^{+} host cells, likely through trogocytosis (Figure 1B).[9, 10] Additionally, circulating TIB-49 cells from blood of WT mice did not express Cd39 despite high levels of this ectoenzyme on the vasculature (Figure 1A), suggesting an essential role of cell-cell contact between acceptor cells and donor cells within the leukemic microenvironment.

TIB-49 cells were then inoculated into WT and *Cd39*$^{-/-}$ mice. Higher levels of TIB-49 cells were detected by FACS in blood and spleen from WT mice than in *Cd39*$^{-/-}$ mice (Figure 1C), and there were delays in engraftment in *Cd39*$^{-/-}$ mice (Figures 1D). TIB-49 cells overexpressing Cd39 with

TdTomato as an indicator (*viz.* TIB-Cd39^{high} cells) were then generated. Compared with parental TIB-49 cells, TIB-Cd39^{high} cells inoculated into WT mice demonstrated faster engraftment (Figure 1E). Further, higher levels of Cd39 on TIB-Cd39^{high} than on TIB-49 cells was confirmed *in vivo* (Supplementary Figure S1D). Importantly, TIB-Cd39^{high} inoculation resulted in more rapid disease progression with shorter times to euthanasia (Figure 1F); albeit proliferation rates of these two cell lines were similar *in vitro* (Supplementary Figure S1E).

We then administered TIB-49-inoculated mice with αCd39 mAb, which was known to deplete Cd39^{high} cells and diminish cell surface Cd39 expression, through FcγRIV-dependent trogocytosis in the MC38 model. [9] Although αCd39 mAb selectively depleted MDSCs and downregulated surface Cd39 expression in multiple immune cells and TIB-49 cells (data was not shown), this form αCd39 mAb monotherapy did not alter the experimental disease course in mice inoculated with either TIB-49 cells or TIB-Cd39^{high} cells (Supplementary Figure S1F). When αCd39 mAb treatment was combined with cytarabine, we found no additional effects in the TIB-49-bearing WT mice (data was not shown). We also tested the effects of αCd39 mAb in TIB-49 chloroma model. In this instance, αCd39 monotherapy effectively boosted chemotherapeutic effects of low dose cytarabine with respect to growth of TIB-49 chloroma *in vivo* (data was not shown). These studies suggest that the benefits and strategy of targeting Cd39 in solid cancer cannot be simply extrapolated to therapeutic applications in liquid cancers, such as in AML.

Bulk RNA-Seq of TIB-49 cells and TIB-Cd39^{high} cells was conducted to explore purinergic and other mechanisms dictating TIB-Cd39^{high} pathogenicity (Supplementary Figure S2A). We found that P2rx1, P2rx7, P2ry10 and P2ry14 were substantively upregulated in TIB-Cd39^{high} cells. We then explored RNA-Sequencing data of human CD39^{+} AML cells in The Cancer Genome Atlas (TCGA) database. We subdivided 151 AML samples into two groups based on median CD39 levels and found that P2RX1 and P2RX7 were upregulated in the group with higher CD39 expression. These increases of P2RX7 were greater than those seen for P2RX1 (Figure 2A). We therefore explored the roles of P2rx7 (*P2rx7-v1* (NM_011027), which is considered the canonical full-length P2rx7) in mediating TIB-49 pathogenicity. FACS detected no P2rx7 protein expression on TIB-49 cells *in vitro*, while these cells after transplantation were found to express higher levels of P2rx7 *ex vivo*. TIB-49 cells overexpressing P2rx7 with TdTomato as an indicator (TIB-P2rx7^{high}) were generated. WT mice were inoculated with TIB-49, TIB-Cd39^{high} and TIB-

P2rx7^{high} cells, respectively. Curiously, the enhanced pathogenicity of TIB-49 cells linked to Cd39 overexpression was replicated by transgenic overexpression of P2rx7 on TIB-49 cells (Figure 2B). *P2rx7* in TIB-49 cells was then deleted by CRISPR (TIB-P2rx7$^{-/-}$ cells, Supplementary Figure S2B), and inoculated into WT mice. The engraftment of TIB-P2rx7$^{-/-}$ cells was significantly delayed when compared with that of TIB-49 cells (Figure 2C), indicating a role of P2rx7 in AML pathogenicity. We tested the efficacy of pharmacological P2rx7 inhibitor A740003. Here too, the survival of standard TIB-49-bearing AML mice in A740003-treated group was significantly prolonged (Figure 2D). However, A740003 was unable to prolong the survival of TIB-Cd39^{high} AML mice (Figure 2E).

P2rx7 was also knocked out in TIB-Cd39^{high} cells by CRISPR (Supplementary Figure S2C) and then inoculated into WT mice. When compared with that of TIB-Cd39^{high} cells, the engraftment of TIB-Cd39^{high}-P2rx7$^{-/-}$ cells was delayed. Times to euthanasia were prolonged with P2rx7 deletion (Figure 2F). These results suggested that Cd39 and P2rx7 may mediate leukemogenic effects via related signaling pathways. Potentially, when the level of (acquired) Cd39 is relatively low on TIB-49 cells, the eATP-mediated P2rx7 pathway may play the dominant role (Figure 2C). However, when the level of (transgenic) Cd39 is high, as on TIB-Cd39^{high} cells, then the nucleotide phosphohydrolysis pathway may take precedence (Figure 2F).

Bulk RNA Seq of TIB-Cd39^{high}-P2rx7$^{-/-}$ cells was conducted to explore putative mechanisms of P2rx7 action in Cd39 mediated pathogenicity (Supplementary Figure S3A). When focusing on the top ten differentially expressed genes (DEGs) in TIB-Cd39^{high}-P2rx7$^{-/-}$, TIB-Cd39^{high} cells *vs.* TIB-49 cells, we found that *Kat6b*, *Nes*, *Fos*, *Ptpn13*, *Zcwpw1* and *Dst* were generally downregulated, while *Wnt6* was upregulated in these two Cd39-overexpressing cells, irrespective of P2rx7 (Figure 3A). When we examined common denominators of Cd39 and P2rx7 pathways by comparing bulk RNA Seq and DEGs of TIB-Cd39^{high} and TIB-P2rx7^{high} cells, we found that *Wnt6* and *Runx2* were upregulated in both TIB-Cd39^{high} and TIB-P2rx7^{high} cells (Figure 3B; Supplementary Figure S3A).

We next performed protein-protein interaction network functional enrichment analysis by using STRING database and Cytoscape software. The results showed that Wnt signaling was identified in the functional networks of DEGs in both TIB-Cd39^{high} cells (Supplementary Figure S3B) and TIB-P2rx7^{high} cells (Supplementary Figure S3C). Therefore, we detected alterations in Wnt acti-

vation. Our results confirmed higher levels of Wnt activation in TIB-Cd39^{high} cells, when compared to TIB-49 cells (Figure 3C).

As Waif1/5T4 inhibited canonical Wnt/β-catenin signaling and activated noncanonical Wnt pathways, [11] we overexpressed human 5T4 (with GFP as an indicator) in various cells via lentiviral vectors (Supplementary Figure 3D). In mice bearing TIB-5T4 cells, overexpression of Waif1 largely abolished disease progression (Figure 3D). Most interestingly, 5T4 significantly prolonged animal survival, even when expressed in the more pathogenic TIB-Cd39^{high} cells (Figure 3E), whereas 5T4^{K76A} mutant had no effect (Figure 3E). Curiously, when expressed in TIB-P2rx7^{high} cells, the protective effect of 5T4 appeared less pronounced (Figure 3E), suggesting Cd39 and P2rx7 may drive differential Wnt- and potentially other pathways in AML. However, when tested, pharmacological Wnt/β-catenin pathway inhibitors (Wnt-C59 and DSMAB) did not show efficacy in the TIB-49 AML model (data was not shown). Future studies are needed to clarify the mechanistic roles of Wnt and 5T4 expression in progression of malignant disease, given ongoing application of experimental targeting of these pathways in both liquid cancers and in solid tumors.

In summary, we describe a novel Cd39-P2rx7-Wnt signaling axis, which serves both as a key determinant of pathogenicity in AML and could be developed further as a therapeutic target. We first found that TIB-49 cells, unlike certain human AML cell lines, [2] were Cd39-negative *in vitro* but did acquire high levels of Cd39 *in vivo*. Heightened AML pathogenicity was associated with Cd39 overexpression. However, therapeutic targeting Cd39 had limited, and hence unexpected, effects in this AML model. Targeting P2rx7 with genetic deletion or pharmacological inhibition resulted in better outcomes in the AML tumor model. Importantly, the overexpression of Cd39 on TIB-Cd39^{high} and P2rx7 on TIB-P2rx7^{high} cells dramatically upregulated the expression of *Wnt6* and *Runx2*. Inhibition of canonical Wnt/β-catenin activation by Waif1/5T4 in these models significantly prolonged AML animal survival, even in the more pathogenic TIB-Cd39^{high} bearing animals.

In conclusion, our study demonstrates that activation of the Cd39-P2rx7 axis enhances pathogenicity of AML cells, at least in part, by recruitment of the associated Wnt/β-catenin signaling pathway (Figure 3F). It is feasible that future anti-leukemia therapies could incorporate the utility of CD39 blockade, P2RX7 inhibition and most crucially the targeting of Wnt/β-catenin signaling pathways.

References

1. Kuek V, Hughes AM, Kotecha RS, Cheung LC. Therapeutic Targeting of the Leukaemia Microenvironment. Int J Mol Sci. 2021;22(13):6888.
2. Aroua N, Boet E, Ghisi M, et al. Extracellular ATP and CD39 Activate cAMP-Mediated Mitochondrial Stress Response to Promote Cytarabine Resistance in Acute Myeloid Leukemia. Cancer Discov. 2020;10(10):1544-1565.
3. Allard B, Longhi MS, Robson SC, Stagg J. The ectonucleotidases CD39 and CD73: Novel checkpoint inhibitor targets. Immunol Rev. 2017;276(1):121-144.
4. Virgilio FD, Vultaggio-Poma V, Sarti AC. P2X receptors in cancer growth and progression. Biochem Pharmacol. 2021;187:114350.
5. Feng L, Cai Y, Zhu M, Xing L, Wang X. The yin and yang functions of extracellular ATP and adenosine in tumor immunity. Cancer Cell Int. 2020;20:110.
6. Feng L, Sun X, Csizmadia E, et al. Vascular CD39/ENTPD1 directly promotes tumor cell growth by scavenging extracellular adenosine triphosphate. Neoplasia. 2011;13(3):206-216.
7. Longhi MS, Feng L, Robson SC. Targeting ectonucleotidases to treat inflammation and halt cancer development in the gut. Biochem Pharmacol. 2021;187:114417.
8. Sun X, Wu Y, Gao W, et al. CD39/ENTPD1 expression by CD4+Foxp3+ regulatory T cells promotes hepatic metastatic tumor growth in mice. Gastroenterology. 2010;139(3):1030-1040.
9. Zhang H, Feng L, de Andrade Mello P, et al. Glycoengineered anti-CD39 promotes anticancer responses by depleting suppressive cells and inhibiting angiogenesis in tumor models. J Clin Invest. 2022;132(13):e157431.
10. Miyake K, Karasuyama H. The Role of Trogocytosis in the Modulation of Immune Cell Functions. Cells. 2021;10(5):1255.
11. Kagermeier-Schenk B, Wehner D, Ozhan-Kizil G, et al. Waif1/5T4 inhibits Wnt/β-catenin signaling and activates noncanonical Wnt pathways by modifying LRP6 subcellular localization. Dev Cell. 2011;21(6):1129-1143.

Figure legends:

Figure 1. TIB-49 cells acquire Cd39 from host cells and levels of Cd39 expression promote TIB-49 AML cells engraftment *in vivo.*

(A) To trace the engraftment of TIB-49 *in vivo*, TIB-49 cells were transduced with TdTomato and then administered intravenously via the tail vein into mice. Altered patterns of Cd39 expression on transplanted TIB-49 cells obtained from blood, spleen, and BM of WT mice and *Cd39*$^{-/-}$ mice.

(B) Schematic diagram depicting proposed trogocytosis and membrane transfer resulting in changes in Cd39 levels on transplanted TIB-49 and recipient cells.

(C) C57BL/6 WT and *Cd39*$^{-/-}$ mice were inoculated with 1×10^6 TIB-49 cells (TdTomato$^+$) through tail vein injection. Quantification of TIB-49 cell percentages in blood, spleen, and BM of TIB-49 inoculated WT and *Cd39*$^{-/-}$ mice were analyzed at Day 31. Data are shown as mean ± SEM. T-test was used for the statistical analysis. **P* < 0.05. ns, not significant.

(D) TIB-49-luciferase/mCherry cells were retro-orbitally inoculated into WT and *Cd39*$^{-/-}$ mice for bioluminescence imaging experiments. When compared with WT mice, leukemia cell engraftment was delayed in *Cd39*$^{-/-}$ mice with decreased disease burdens.

(E) TIB-49 and TIB-Cd39^{high} cells proportions in blood, splenocytes and BM of WT mice were analyzed at Day 19.

(F) Survival of TIB-49 (n=9) and TIB-Cd39^{high} (n=10) bearing mice was compared. The log-rank test was used for statistical analyses.

Figure 2. Modulation of P2rx7 signaling impacts Cd39 associated pro-leukemogenic effects *in vivo*. TIB-Cd39^{high} and TIB-P2rx7^{high} cells showed enhanced pathogenicity in WT mice, while P2rx7 deletion in TIB-49 and TIB-Cd39^{high} cells delayed engraftment of leukemic cells. Pharmacological P2rx7 inhibitor prolonged the survival of TIB-49-bearing AML mice, not TIB-Cd39^{high} AML mice.

(A) Quantification of selected P2 receptor expression, in 151 human AML samples in TCGA database, with high or low expression of CD39 relative to the median expression level. Mann-Whitney test was used for statistical analysis. **P* < 0.05, *****P* < 0.0001.

(B) C57BL/6 WT mice were inoculated with TIB-49, TIB-Cd39^{high} or TIB-P2rx7^{high} cells, respectively through tail vein injection. Time to euthanasia compared of mice inoculated with TIB-

49 (n=11), TIB-Cd39^{high} (n=12) or TIB-P2rx7^{high} cells (n=6). The log-rank test was used for statistical analyses. TIB-Cd39^{high} and TIB-P2rx7^{high} cells showed enhanced pathogenicity in WT mice.

(C) C57BL/6 WT mice were inoculated with TIB-49 cells or TIB-P2rx7$^{-/-}$ cells, respectively through tail vein injection. Times to euthanasia of mice inoculated with TIB-49 (n=15) or TIB-P2rx7$^{-/-}$ cells (n=15) was then compared. The log-rank test was used for statistical analyses. P2rx7 deletion in TIB-49 cells delayed engraftment in WT mice.

(D, E) C57BL/6 WT mice were inoculated with 1×10^6 TIB-49 cells or TIB-Cd39^{high} cells through tail vein injection. Mice received 50 mg/kg P2rx7 antagonist A740003 or DMSO vehicle treatment from day 15 every other day for 14 days. Time to euthanasia of mice bearing TIB-49 cells (n=15 in each group) or TIB-Cd39^{high} cells (n=10 in each group) was compared. Log-rank test was used for statistical analyses. Benefits potentially seen with A740003 alone for TIB-49 cells, were not noted in the TIB-Cd39^{high} group.

(F) C57BL/6 WT mice were inoculated with TIB-Cd39^{high} cells or TIB-Cd39^{high}-P2rx7$^{-/-}$ cells respectively through tail vein injection. Times to euthanasia of mice inoculated with TIB-Cd39^{high} cells (n=10) or TIB-Cd39^{high}-P2rx7$^{-/-}$ cells (n=10) were contrasted. The log-rank test was used for statistical analyses and indicated benefit of genetic deletion of P2rx7 in these cells.

Figure 3. Downstream Wnt/β-catenin signaling mediates Cd39 and P2rx7 pro-leukemogenic effects *in vivo*. Wnt-activated inhibitory factor 1 (Waif1/5T4) significantly prolonged TIB-49 and TIB-Cd39^{high} cells bearing animal survival. When expressed in TIB-P2rx7^{high} cells, the protective effect of 5T4 appeared less pronounced.

(A) Top ten common DEGs of TIB-Cd39^{high} cells and TIB-Cd39^{high}-P2rx7$^{-/-}$ cells, when compared with native TIB-49 cells. Data are shown as mean ± SEM (n=3). T-test was used for the statistical analysis. ***$P < 0.001$.

(B) *Wnt6* and *Runx2* transcript expression patterns on TIB-49 cells, TIB-Cd39^{high} cells and TIB-P2rx7^{high} cells.

(C) Wnt activation in TIB-Cd39^{high} cells. TIB-49 and TIB-Cd39^{high} cells were transfected with Wnt-EGFP indicator or reporter plasmid. TIB-Cd39^{high} cells show increased levels of Wnt activation.

(D) C57BL/6 WT mice were inoculated with 1×10^6 syngeneic TIB-49 (n=5) or TIB-5T4 cells (n= 4). Times to euthanasia of mice in these two groups were analyzed with the log-rank test, indicating benefits of Wnt inhibition.

(E) C57BL/6 WT mice were inoculated with 1×10^6 syngeneic TIB-Cd39^{high} cells (n=21), TIB-Cd39^{high}-5T4 cells (n=9), TIB-P2rx7^{high} cells (n=8), TIB-P2rx7^{high}-5T4 cells (n=10) and TIB-Cd39^{high}-5T4^{K76A} (loss of function) cells (n=5) respectively. Survival of mice was analyzed with the log-rank test, confirming benefits of active Waif1/5T4 expression in these experimental models, targeting TIB-Cd39^{high} or TIB-P2rx7^{high} cells. $*P < 0.05$; $**P < 0.01$, $****P <0.0001$.

(F) Depiction of the Cd39-P2rx7 axis and Wnt/β-catenin signaling pathways in proposed mediation of AML model pathogenicity.

Figure 1

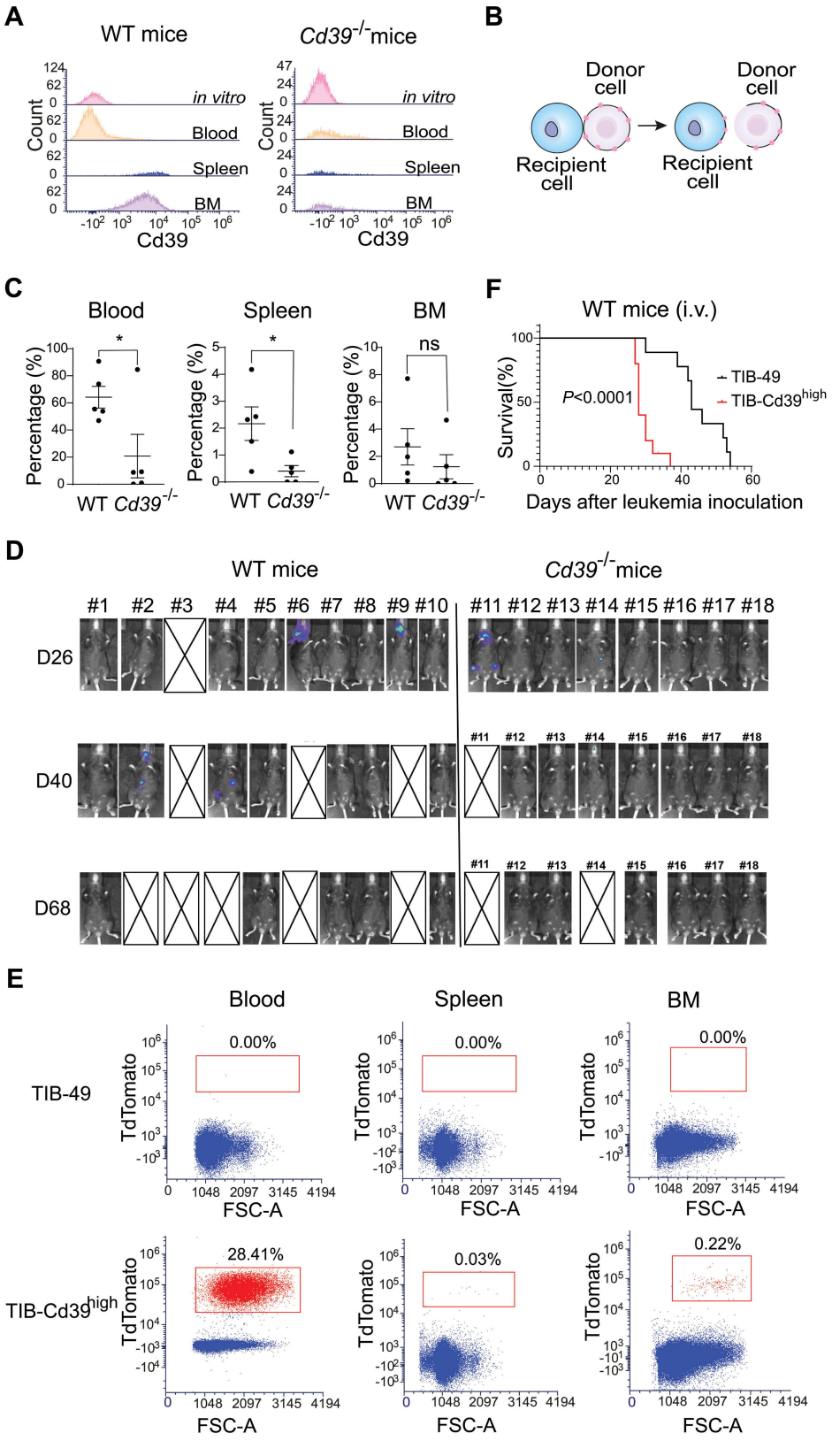
A
WT mice
Cd39-/- mice
Count
in vitro
Blood
Spleen
BM
Cd39
B
Donor cell
Recipient cell
C
Blood
Spleen
BM
Percentage (%)
ns
WT Cd39-/-
F
WT mice (i.v.)
Survival(%)
P<0.0001
TIB-49
TIB-Cd39high
Days after leukemia inoculation
D
WT mice
Cd39-/- mice
D26
D40
D68
E
TIB-49
TIB-Cd39high
TdTomato
FSC-A
0.00%
28.41%
0.03%
0.22%

Figure 2

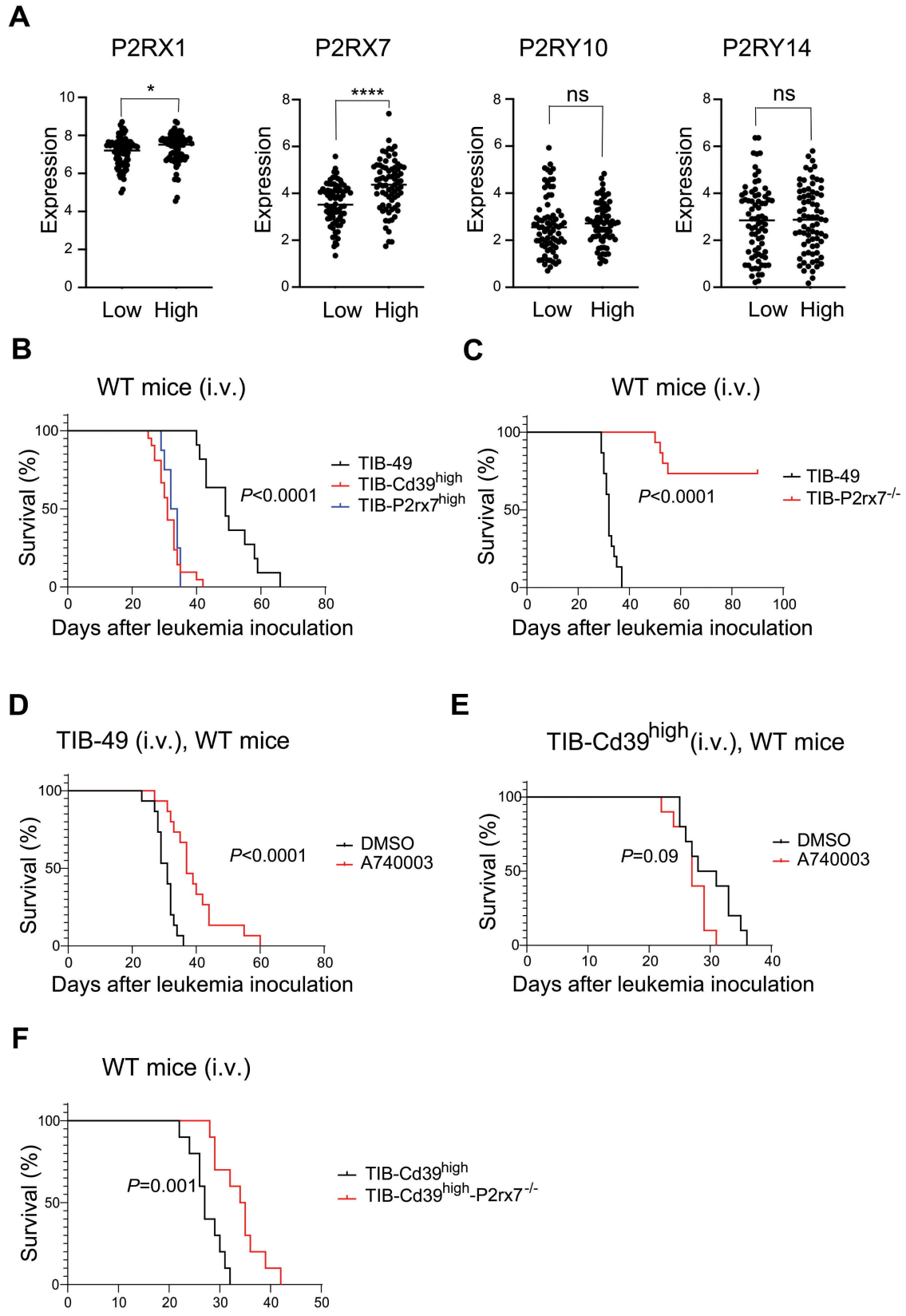
A
P2RX1
P2RX7
P2RY10
P2RY14
Expression
*
****
ns
ns
Low
High
B
WT mice (i.v.)
Survival (%)
Days after leukemia inoculation
P<0.0001
TIB-49
TIB-Cd39high
TIB-P2rx7high
C
WT mice (i.v.)
P<0.0001
TIB-49
TIB-P2rx7-/-
D
TIB-49 (i.v.), WT mice
P<0.0001
DMSO
A740003
E
TIB-Cd39high(i.v.), WT mice
P=0.09
DMSO
A740003
F
WT mice (i.v.)
P=0.001
TIB-Cd39high
TIB-Cd39high-P2rx7-/-

Figure 3

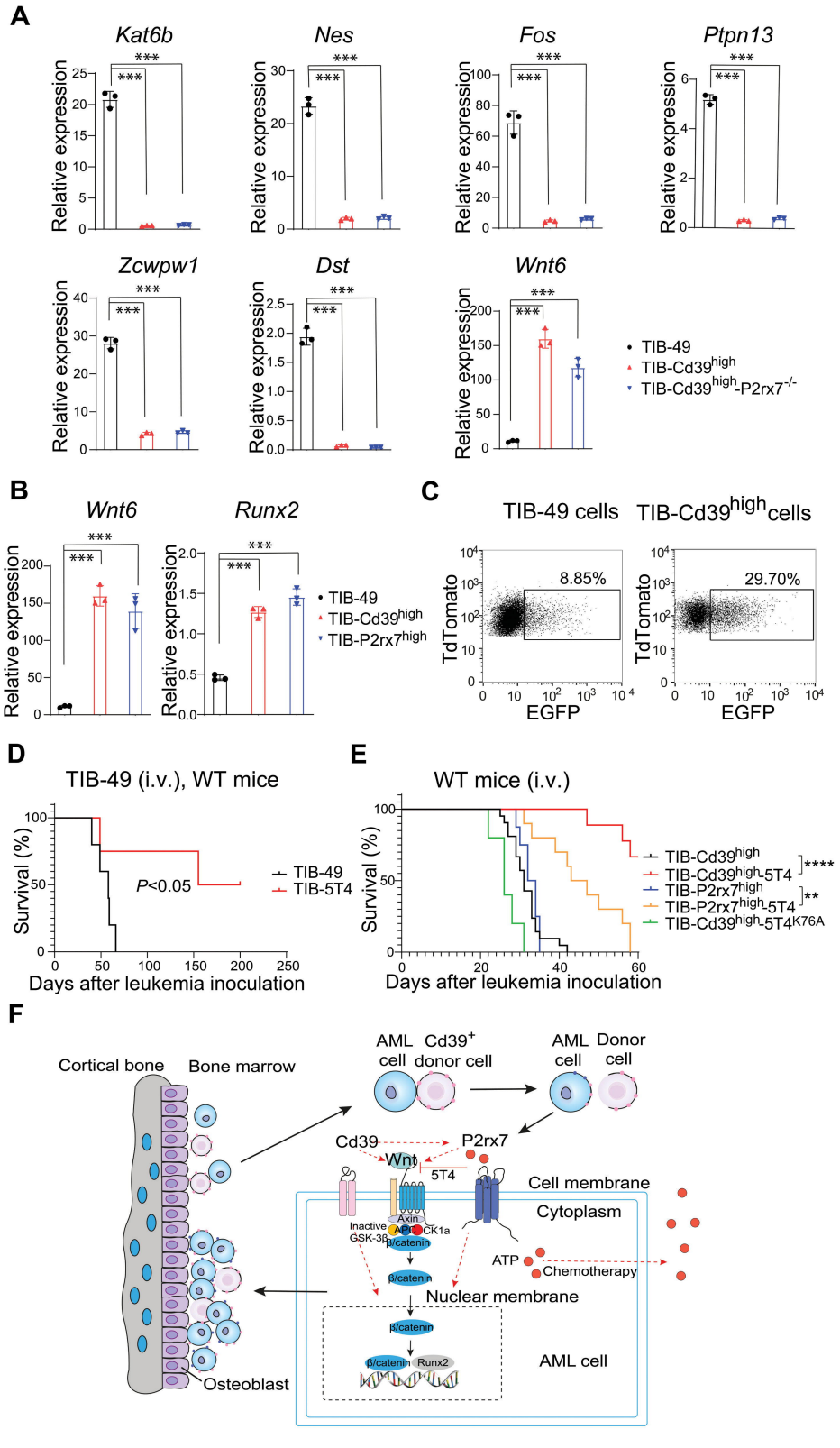
A
Kat6b
Nes
Fos
Ptpn13
Zcwpw1
Dst
Wnt6
Relative expression
***
TIB-49
TIB-Cd39high
TIB-Cd39high-P2rx7-/-
B
Wnt6
Runx2
TIB-49
TIB-Cd39high
TIB-P2rx7high
C
TIB-49 cells
TIB-Cd39high cells
8.85%
29.70%
TdTomato
EGFP
D
TIB-49 (i.v.), WT mice
Survival (%)
P<0.05
TIB-49
TIB-5T4
Days after leukemia inoculation
E
WT mice (i.v.)
TIB-Cd39high
TIB-Cd39high-5T4
TIB-P2rx7high
TIB-P2rx7high-5T4
TIB-Cd39high-5T4K76A
****
**
F
Cortical bone
Bone marrow
AML cell
Cd39+ donor cell
Donor cell
Cd39
P2rx7
Wnt
5T4
Cell membrane
Cytoplasm
Axin
Inactive GSK-3β
CK1a
β/catenin
ATP
Chemotherapy
Nuclear membrane
Runx2
AML cell
Osteoblast

Supplementary Figure Legends:

Supplementary Figure S1. Cd39 expression on immune cell *in vivo* and on TIB-49 cells *in vitro*. Targeting Cd39 by αCd39 mAb did not delay AML disease course inoculated with either TIB-49 cells or TIB-Cd39^{high} cells.

(A) C57BL/6 WT mice were inoculated with 1×10^6 syngeneic TIB-49 (TdTomato$^+$) cells via tail vein injection. Blood, splenocytes and BM from control and test mice were collected. Single-cell suspensions were prepared and Cd39 expression levels on immune cells were analyzed by FACS.

(B) Cd39 expression on TIB-49 cells *in vitro* was analyzed by FACS. CHO-Cd39 cells were used as positive control.

(C) Cd39 transcript expression (97 bp PCR amplicon) on cultured TIB-49 cells (Sample 1) and TIB-49 cells sorted from spleen (Sample 3) and BM (Sample 4) of leukemia bearing WT mice. TIB-Cd39^{high} transgenic cells (Sample 2) were used as positive control. β-actin was used as internal reference.

(D) Levels of membrane Cd39 expression at Day 26 on TIB-49 cells and immune cells in the spleen and BM of TIB-49 *vs.* TIB-Cd39^{high} cells inoculated into WT mice.

(E) TIB-49 cells and TIB-Cd39^{high} cells were cultured in 96-well plate. Cellular proliferation expressed as measured by CCK8 after cultures for 24 h, 48 h and 72 h, respectively.

(F) C57BL/6 WT mice were inoculated with 1×10^6 syngeneic TIB-49 or TIB-Cd39^{high} cells through tail vein injection. Mice received 5 mg/kg CTRL or αCD39 mAb treatment at Days 18, 21, 24 and 27 respectively. Time to euthanasia of mice bearing TIB-49 cells (n=14 in each group) or TIB-Cd39^{high} cells (n=10 in each group) was compared. The log-rank test was used for statistical analyses.

Supplementary Figure S2. Volcano plots of TIB-Cd39^{high} cells, and strategy for P2rx7 deletion in TIB-49 cells and TIB-Cd39^{high} cells by CRISPR.

(A) Bulk RNA-Seq was conducted on TIB-49 cells and TIB-Cd39^{high} cells. Volcano plots are presented showing "differently expressed genes" (DEGs) between these two cell lines.

(B) To establish TIB-P2rx7$^{-/-}$ cells, 50 nt was deleted in allele_1 and 7 nt was inserted; in addition, 38 nt was deleted in allele_2 and 13 nt was inserted. These resulted in early termination of P2rx7 translation, with no functional protein detected.

(C) To establish TIB-Cd39^{high}-P2rx7$^{-/-}$ cells, 23 nt were deleted in allele _1 and 13 nt deleted at gene allele_2. Both resulted in early termination of P2rx7 translation, and no functional protein was produced.

Supplementary Figure S3. Volcano plots of TIB-Cd39^{high}-P2rx7$^{-/-}$cells and TIB-P2rx7^{high} cells. Wnt signaling was identified in the functional networks of DEGs in both TIB-Cd39^{high} cells and TIB-P2rx7^{high} cells. 5T4 expression on multiple cells.

(A) Bulk RNA-Seq was conducted on TIB-Cd39^{high}-P2rx7$^{-/-}$cells and TIB-P2rx7^{high} cells. Volcano plots are presented showing DEGs between cell lines.

(B-C) Protein-protein interaction networks of the top two thousand DEGs in TIB-Cd39^{high} (B) and TIB-P2rx7^{high} cells (C). These networks were constructed with > two nodes with interaction confidence values >0.90.

(D) 5T4 expression on TIB-5T4, TIB-CD39^{high}-5T4 and TIB-P2rx7^{high}-5T4 cells, as confirmed by FACS.

Supplementary Figure S1

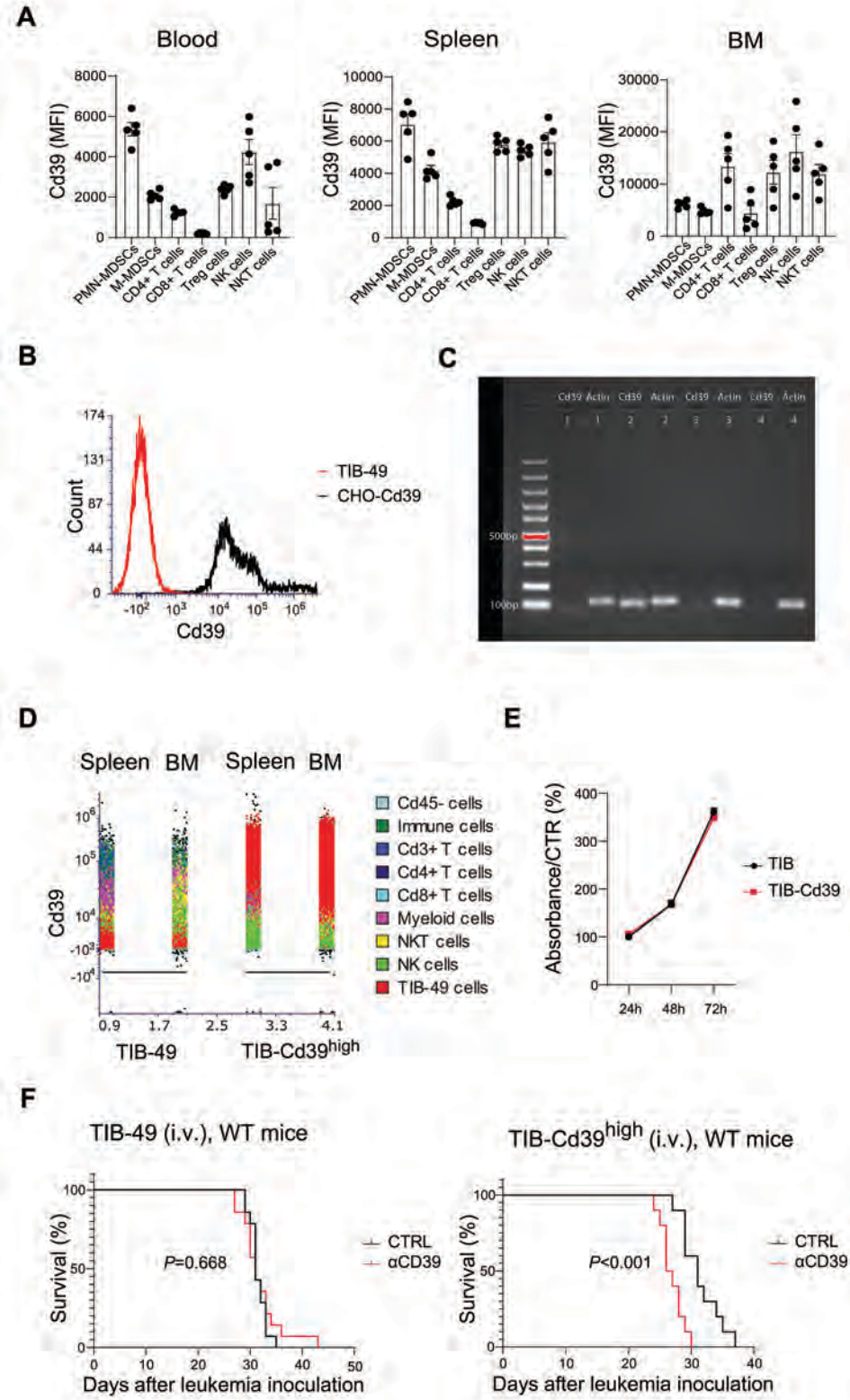

Supplementary Figure S2

A

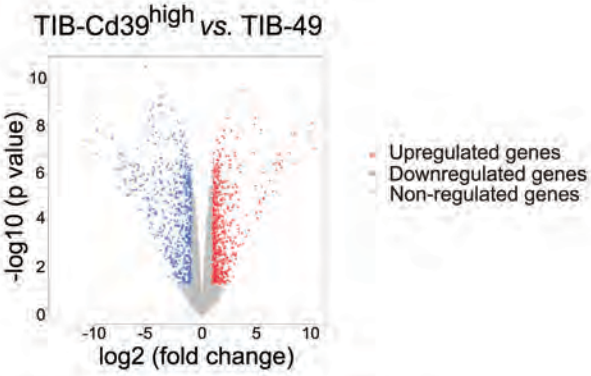

B WT allele

```
GGTGAGCGATAAGCTGTACCAGCGGAAAGAGCCTGTTATCAGCTCCGTGCACACCAAGGTCAAAGGCATAGCAGAGGTGACGG
AGAATGTCACAGAGGGTGGGGTGACGAAGTTAGGACACAGCATCTTTGACACTGCAGACTACACCTTCCCTTTG
.ValSerAspLysLeuTyrGlnArgLysGluProValIleSerSerValHisThrLysValLysGlyIleAlaGluValThrG
luAsnValThrGluGlyGlyValThrLysLeuGlyHisSerIlePheAspThrAlaAspTyrThrPheProLeu...
```

KO allele_1: 50 nt deletion, 7 nt insertion

```
GGTGAGCGATAAGCTGTACCAGCGGAAAGAGCCTGTTATCAGCTCCGTGCACA.....................TCAGCTC.
.....................GTGACGAAGTTAGGACACAGCATCTTTGACACTGCAGACTACACCTTCCCTTTG
..SerAspLysLeuTyrGlnArgLysGluProValIleSerSerValHisIleSerSerEnd
```

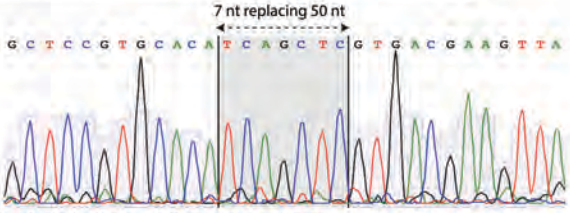

KO allele_2: 38 nt deletion, 13 nt insertion

```
GGTGAGCG.............GCTCCGTGCACGT.............GTGCACACCAAGGTCAAAGGCATAGCAGAGGTGACGG
AGAATGTCACAGAGGGTGGGGTGACGAAGTTAGGACACAGCATCTTTGACACTGCAGACTACACCTTCCCTTTG
.ValSerGlySerValHisValCysThrProArgSerLysAlaEnd
```

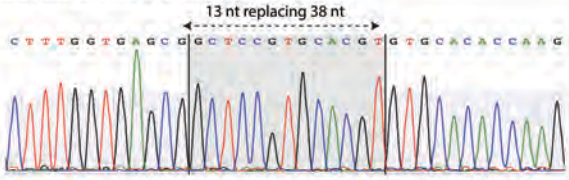

C WT allele

```
TAAGCTGTACCAGCGGAAAGAGCCTGTTATCAGCTCCGTGCACACCAAGGTCAAAGGCATAGCAGAGGTGACGGAGAATGTCA
.LysLeuTyrGlnArgLysGluProValIleSerSerValHisThrLysValLysGlyIleAlaGluValThrGluAsnVal.
```

KO allele_1: 23 nt deletion

```
TAAGCTGTACCA.....................CCGTGCACACCAAGGTCAAAGGCATAGCAGAGGTGACGGAGAATGTCA
.LysLeuTyrHisArgAlaHisGlnGlyGlnArgHisSerArgGlyAspGlyGluCysHisArgGlyTrpGlyAspGluValA
rgThrGlnHisLeuEnd
```

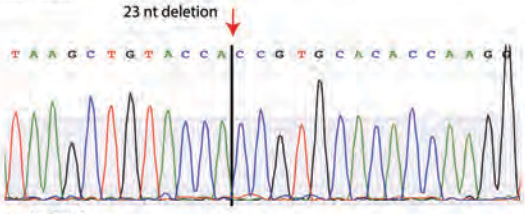

KO allele_2: 13 nt deletion

```
TAAGCTGTACCAGCGGAAAGAGCCTGTTATCAGC.............AGGTCAAAGGCATAGCAGAGGTGACGGAGAATGTCA
.LysLeuTyrGlnArgLysGluProValIleSerArgSerLysAlaEnd
```

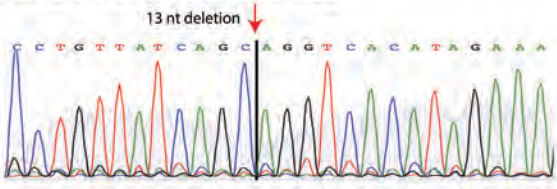

Supplementary Figure S3